

SPECIFIC ASPECTS ON CRACK ADVANCE DURING J-TEST METHOD FOR STRUCTURAL MATERIALS AT CRYOGENIC TEMPERATURES

Klaus Weiss and Arman Nyilas
Forschungszentrum Karlsruhe
Institute for Technical Physics
D-76021 Karlsruhe, Germany
klaus.weiss@itp.fzk.de, arman.nyilas@itp.fzk.de

Abstract

Cryogenic elastic plastic, J-Integral investigations on metallic materials show often negative crack extension values with respect to resistance curve J-R. According to the present ASTM standard the use of unloading compliance technique relies on the estimation procedure of the crack lengths during the unloading sequences of the test. The current standard, however, does not give any specific procedure for treating such negative data. To date the applied procedure by several laboratories uses the shifting of the negative crack extension values either to the onset of the blunting line or to the offset of the resistance curve. The present paper represents a solution of the negative crack length problem based on a mechanical evaluation procedure of the unloading slopes. In addition, this work deals with the crack tunneling phenomenon, observed for high toughness materials and shows the suppressing of this crack extension appearance by using electro discharge machining (EDM) side-groove technique instead of side-groove machining operation. The achieved progress using this evaluation technique is demonstrated on different materials such as cryogenic high toughness stainless steels, low carbon ferritic steel and aluminum alloys from the series of 7000 and 5000.

Introduction

Deeply cracked Compact Tension (CT) standard specimens of high toughness materials show during loading a plastic response if the size of specimen doesn't meet the plane strain fracture toughness requirements fixed by the ASTM standard E 399 [1]. To ensure an applicable solution for small specimens of high toughness materials the ASTM standard test method E 813-81 [2] was developed in the early 80's. This widely used test method considers the J-Integral contour, a surface integral, characterizing the stress-strain field around the crack tip. During this initial version of the standard the critical J-value was estimated by determining the onset of the crack extension start after the blunting of the initiated fatigue crack. For this reason the intersection of tearing line and the drawn material's blunting line was determined using the resistance curve J-R. This specific intersection point defines a physical meaningful value, because during the loading of the cracked specimen the crack advance starts only after blunting of the preexisting fatigue crack. At present, the revised standard E 813 approved at 1988 [3] makes use of a small crack extension portion, derived by the blunting line shift of 0.2 mm and its intersection with the power line regression function of the tearing curve. In this standard the critical J-value is defined as an engineering estimate of the J-integral value, which is requested to produce a small amount of a stable crack extension of 0.2 mm.

Consequently, the ASTM standard E 813-88 [3] specifies two equivalent procedures, which can be used for the determination of the resistance curve J-R. These are the *Multiple-Specimen Technique* (described in § 8.3) and the *Single-Specimen Technique* (§ 8.4). The *Multiple-Specimen Technique* is so far simple and arise no problems for the direct estimation of the crack extension lengths after heat tinting and breaking of the specimen. This elaborate technique has, however, the disadvantage of the required high number of specimens.

Therefore, with *Single-Specimen Technique* it is possible to measure the critical J by subdividing the load displacement curve into several parts with small unloading / reloading processes. The J-value of each part can be easily calculated. The major difficulty, however, is the corresponding crack length determination at each unloading point, which relies on a general compliance function. According to type of material, temperature, and specimen size it may happen that the obtained crack length values are negative. Especially measurements in cryogenic regime show a high amount of negative values. Owing to the virtual negative crack extension estimates, the J-R curve determined by the single specimen test method shows the peculiarity of decreasing the crack lengths during the initial loading sequence. The ASTM standard, however, does not specify any procedure with respect to this problem. Until to date several laboratories exclude the negative data by simply shifting according to their own expertise. Naturally, there were several attempts to achieve a general solution of this problem by different research groups. This phenomenon has been treated by Rosenthal *et al.* [4] with an analysis procedure of the data fit and a mathematically defined crack length shift along the physical crack length abscissa avoiding the operator bias. In a recent paper by Seok [5] the theoretical compliance function has been corrected using the idea of the possible compressive residual stresses ahead of the crack tip. The compliance correction function has been shown that at least for ambient temperature measurements the procedure delivers so far reliable results.

The present paper is the result of observations during several tests conducted by Nyilas *et al.* [6] and Nishimura *et al.* [7] in cryogenic regime near liquid helium temperature. The negative crack growth is related to the stiffness changes of the specimen during loading and is the consequence of the crack tip blunting of the virgin specimen and the strain hardening of the plastic zone ahead of the crack tip. The specimen's initial stiffness determined at the zero offset increases soon after passing the micro-elastic limit. The reason for this is at first the starting of the blunting process at the crack tip and at second the specimen deformation owing to the partly plane stress condition. In fact, the specimen loaded for the J-test procedure has a mixed mode character with respect to stress-strain field behavior. According to the size of the specimen the sample preserves in the centrally located region its plane strain condition, whereas the two sides have at the near surface a plane stress condition. Therefore, the crack profile shows after specimen breaking according to the toughness level of the material and the specimen size more or less a Gaussian distribution profile (crack tunneling). These both processes gradually increase the stiffness and only after the crack initiation the stiffness starts to decrease. This means that there are two mechanisms, which determine the value of the stiffness depending on the load line displacement position. Consequently, these two opposing processes modeled as a mathematical function result in a maximum or a minimum.

In addition, the determined crack extension lengths having negative values are coupled with a considerable scatter in spite of high precision measurement. In general, in such cases owing to the lack of a recommendation by standards the crack lengths are shifted by individual engineering judgment. The recent Japanese standard JIS Z 2284 [8], the only

existing standard applicable at low temperatures recommends a correction by moving the entire data along the crack extension axis to coincides with the blunting line. So far this recommendation is a solution but without a reasonable explanation. Therefore, to avoid a biased data selection and to obtain a satisfactory solution towards a reasonable critical J-value assessment a new approach has been developed for the shifting the J-R plots by seeking the crack initiation point. The initial evaluations regarding this new procedure have been represented by Nyilas *et al.* [9] for a number of high toughness materials tested in cryogenic regime.

Materials and experimental setup

The materials used for these cryogenic mechanical J-Integral investigations are as follows: A Russian high strength cryogenic stainless steel 20 mm thick plate material designated as 03Cr20Ni16Mn6N and aged at 973 K for 200 h, a cast stainless steel with Werkstoff No. 1.3960, an extruded aluminum alloy bar of 80 mm Ø of material 7075 T-6, an aluminum alloy 5059 as a 5 mm thick plate, an aluminum alloy 5083 as 10 mm thick plate, and a ferritic steel (ST 52). These measurements were carried out at 295 K, 77 K, or at 7 K using the cryogenic test facility described in the paper given by Nishimura *et al* [10]. The specimens were ASTM proportional compact tension type with thicknesses between 4 and 25 mm and widths between 36 and 50 mm. The displacement measurements are performed by using a high resolution cryogenic proof extensometer (see Sugano *et al* [11]).

Measurements, discussion, and results

At initial stage of the measurements the material 03Cr20Ni16Mn6N has been investigated with four CT specimens of 5 mm thickness. The specimens No 1 and 2 (Uag5-1 and Uag5-2) have been measured according to the ASTM standard [3]. The original stiffness data obtained from the unloading data has been plotted against the onset of the load line displacement values as shown in Fig.1. Prior to the next measurements the experimental plots of these tests were smoothed by a 2nd order least square regression. The maximum of stiffness in this plot (Fig. 1) represents the important parameter of crack initiation. The next two tests with same material were carried out by observing the maximum position of the stiffness. The loading of the specimen No 3 was stopped directly in the vicinity of the maximum, whereas the No 4 was loaded slightly more than the former one. As shown in Fig. 1 the maximum of the stiffness confirms the onset of the crack start, showing some void coalescence ahead of the fatigue pre-crack tip. The images at right show clearly this evidence. During the initial stage of the loading the stiffness of the specimen increases as given by the Fig. 1. At further loading after micro-void coalescence, crack advance starts and beyond this point the stiffness begins to decrease. This phenomenon was confirmed with several tests where the unloading/loading process was stopped at the maximum stiffness point. The analyzed fractured CT specimens confirm the observation and therefore the maximum stiffness point has to be declared as the crack initiation point. In addition, the actual physical crack lengths have been calculated by the determined smooth unloading stiffness function using the maximum stiffness as zero point and the last stiffness as the terminal point of the crack length determined after specimen fracturing. Hereafter, the J-R curve was established by setting the corresponding J-value of the maximum stiffness position to 0-offset blunting line and plotting the subsequent crack lengths into the diagram as shown in Fig. 2. The diagram in Fig.2 at left gives the calculated data of the crack lengths determined with the actual compliance function.

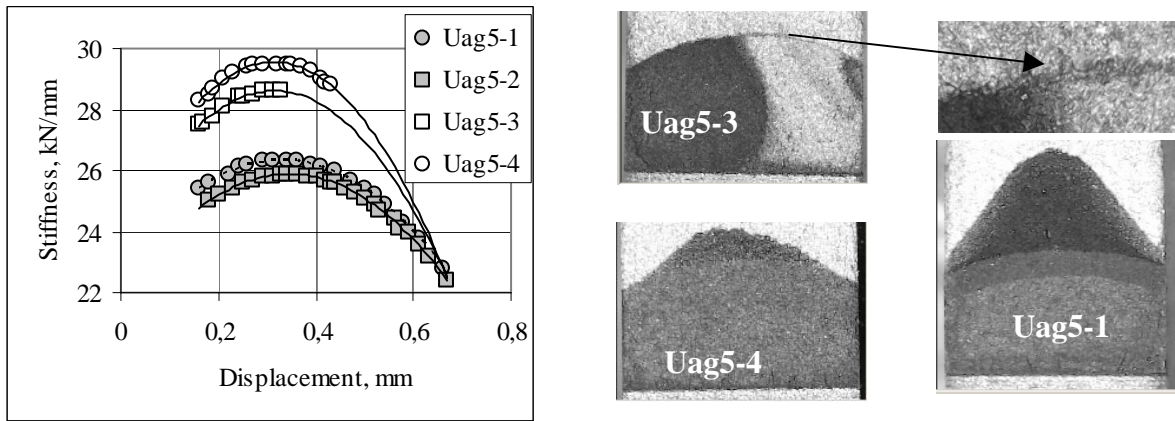


FIGURE 1. Unloading line slopes versus load line displacement of unloading onset positions of 4 different measurements with the material 03Cr20Ni16Mn6N at 7 K. The drawn lines are the 2nd order regression line curves of each specimen. The images at right show the fracture appearance of crack initiation phase, crack start, and the crack extension of these 5 mm thick compact tension specimens. The arrow indicates the void coalescence ahead of crack tip.

As evident, the achieved total physical crack extension length calculated according to the compliance function differs from the observed physical crack length of the broken specimen. Therefore, considering the measured final physical crack length and the fatigue pre-crack length the data are normalized using the smoothed parabolic function to real crack lengths as given in J-R diagram at right (Fig. 2). The obtained result with respect to provisional critical J-value of this investigated material is given in Table 1 according to the described evaluation procedure.

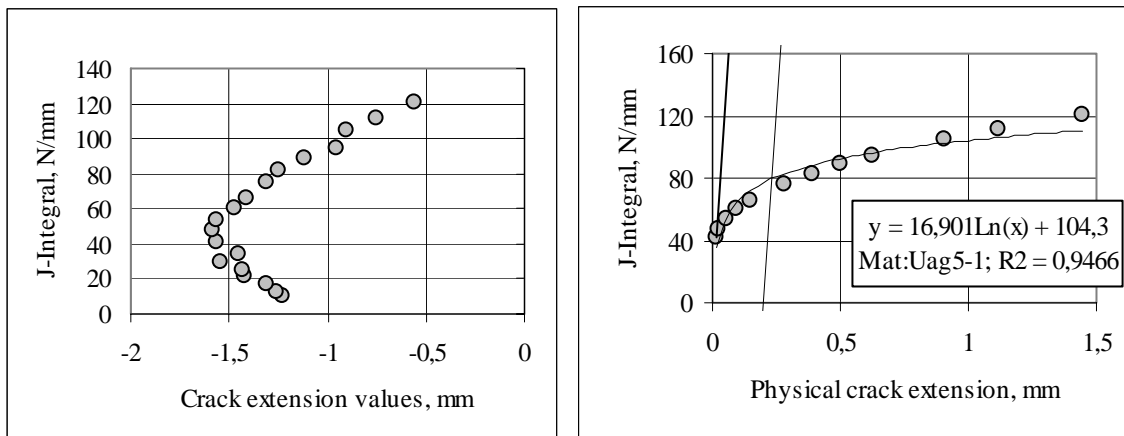


FIGURE 2. The diagram at left shows the original J versus physical crack extension plots (material: 03Cr20Ni16Mn6N) determined by the compliance function EBC versus a/W , where E the Young’s modulus, B thickness of the specimen, C compliance of the unloading line, W width of the specimen, and a as the determined crack length. The diagram at right shows the resistance curve of this material measured at 7 K with the evaluated critical J-value. The intercept of the derived power function with the 0.2 mm shifted blunting line gives the provisional critical J-value.

Figure 3 shows within this context the complete load versus displacement plots of the specimen No 1 of the Russian steel measured at 7 K and indicates also the discontinuous yielding (diagram at right) of the curve between the two unloading lines, which has to be

recognized by the used software as a serration and not as an unloading sequence. The data of the unloading lines acquired with a sampling rate of 60 Hz have been computed as a 1st order regression line. Prior to the computation 3 % of the upper and bottom data have been rejected to avoid any nonlinearity effects.

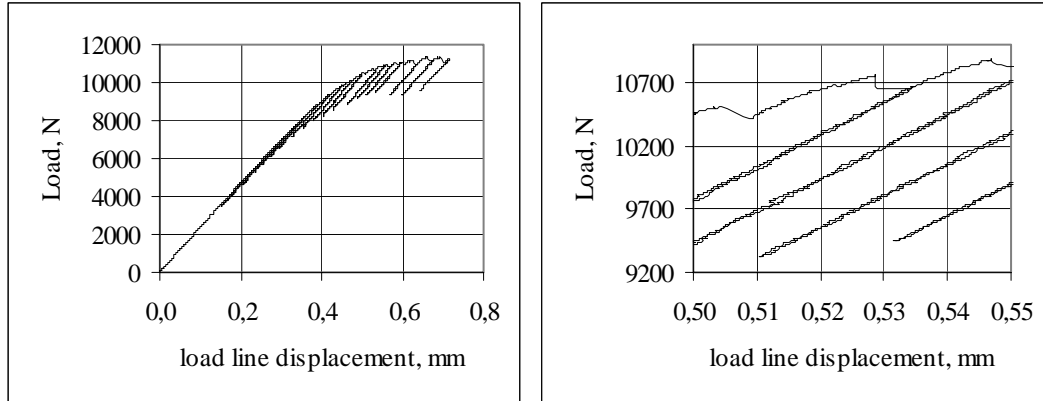


FIGURE 3. Load versus displacement curve of the material 03Cr20Ni16Mn6N measured at 7 K (diagram at left) shows for specimen No 1 the unloading lines in larger magnification (diagram at right) with some low temperature bound discontinuous yielding (serrations) between the unloading sequences. Specimen (Uag5-1) details are as follows: W = 36 mm, B = 5 mm, specimen notch position = 16.75 mm, fatigue pre-crack length = 19.70 mm, physical crack extension = 21.13 mm

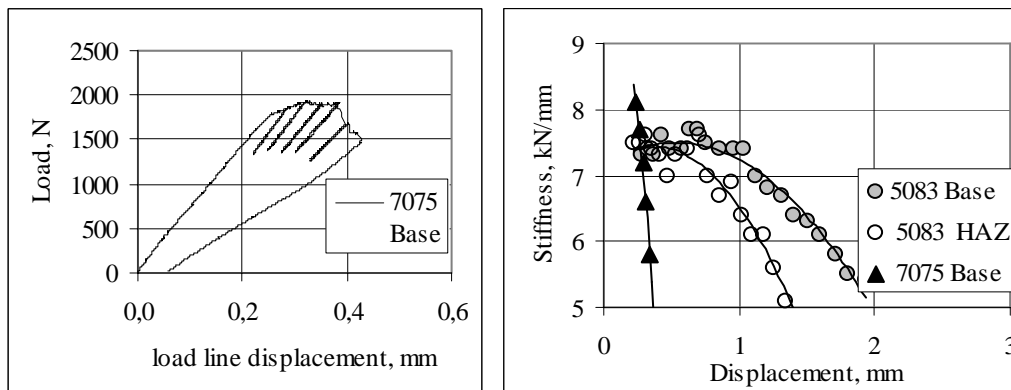


FIGURE 4. Load versus load line displacement of the material 7075 measured at 7 K with the unloading compliance lines. The diagram at the right side shows the unloading slopes of the loading/unloading plots for material 7075 as well as for the material aluminum 5083 in base and HAZ (heat affected zone) condition.

To confirm the findings further, different class of materials were selected to measure the critical J using the described procedure. The aluminum alloy of the series 7075 T6 was measured in two orientations, transverse and longitudinal. Figure 4 shows the load versus displacement diagram of this alloy obtained at 7 K in longitudinal orientation. The diagram at right shows the stiffness plots of alloy 7075 along with aluminum alloy 5083 (base and HAZ). As evident the low toughness materials have the tendency of an immediate stiffness decrease upon loading. This maximum position coincides also with the crack initiation. This finding is also verified with the aluminum alloy 5059, measured at 295 K as shown in Fig.5. The evaluated critical J values of these materials are given in Table 1. In addition, the Al alloy 7075 has been also measured directly at 7 K with a 15 mm thick CT specimen using the ASTM standard E 399. The valid K_{IC} value matches exactly within less than 1 % scatter with the converted K_{IC} of the determined J_{IC} result given in Table 1.

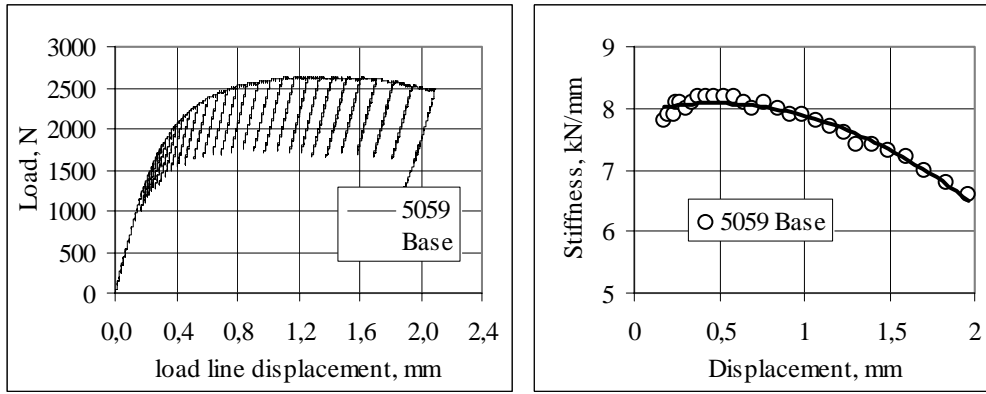


FIGURE 5. Load versus load line displacement of the aluminum alloy 5059 measured at 295 K with the unloading compliance lines. The diagram at right shows the obtained stiffness data of the loading/unloading plots. The drawn line is the regression function of the plots.

One major drawback with all these experiments carried out with small size specimens is the crack tunnelling. The observed large crack tunnelling phenomenon (see Fig.1) often violates the validity criterion specified by the standards. To investigate this behaviour we selected a high toughness stainless steel cast material (Werkstoff No: 1.3960). The small 4 mm thick CT specimens for these measurements were prepared prior to fatigue pre-cracking with 0.5 mm deep EDM side-grooves, thus introducing a very sharp notch radius of 0.1 mm. The effective thickness of the ready specimen was 3 mm. The fatigue pre-crack profile achieved at 7 K prior to the J-test show at the specimen surface even a higher pre-crack length compared to the centre region of the specimen. Figure 6 shows the J-R diagram of the specimen No 1 investigated at 7 K. Although the determined critical J-value of this near surface specimen is very high with 378 N/mm the image at right shows no crack tunnelling due to the sharp EDM notch along the two paths onto the surface of the specimen. The far right image of Fig. 6 shows the investigation result performed at 7 K of the cast material from another batch. The crack profile of this specimen with $B = 25$ mm shows, however, a crack tunnelling although the CT specimen had a 90° machine side-groove. The determined J-value of this test is ~ 580 N/mm and far from validity, whilst the small CT specimen yields to a provisional J-Integral close to a valid value.

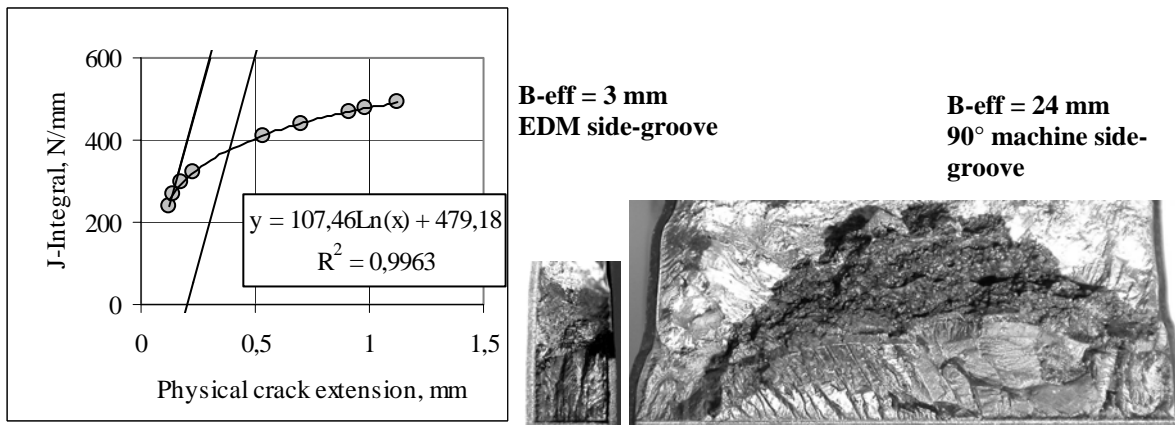


FIGURE 6. Resistance curve of the cast stainless steel material (Werkstoff No: 1.3960) measured at 7 K shows the evaluated critical J-value. Details of the specimen are as follows: Compact tension specimen with $B = 4$ mm (side grooved by EDM machining), B -effective = 3 mm, and $W = 36$ mm. The images at right show the fracture appearance of the measured 2 specimens one with B -effective 3 mm (EDM side-groove) and the other one with B effective = 24 mm (90° machine side-groove).

TABLE 1. Determined critical J-Integral data of various materials at different temperatures

Material & condition	Temp. K	J _{IC} N/mm	Material & condition	Temp. K	J _{IC} N/mm
03Cr20Ni16Mn6N	7	80 / 77	Al 7075 long	7	9
Al 5083 base	295	45 / 43	Al 7075 trans.	7	27
Al 5083 base	77	70 / 64	Al 5059 plate	295	56
Al 5083 base	7	42 / 43	Al 5059 plate	77	78
Al 5083 weld	295	46 / 53	Al 5059 plate	7	20
Al 5083 weld	77	63 / 67	1.3960	7	378
Al 5083 weld	7	29 / 31	1.0570 (ST 52)	295	50

To scrutinize further the effect of EDM-side groove on crack profile we selected a common ferritic material (Werkstoff 1.0570, designated as ST 52) to perform J-integral measurements at 295 K using different size and type CT specimens. The yield and tensile strengths of this material at 295 K are determined as 285 MPa and 579 MPa, respectively. The details of the prepared three specimens were as follows: CT-1 with 4 mm thickness, 36 mm width having no side-groove; CT-2 with 25 mm thickness, 50 mm width having no side-groove; CT-3 with 4 mm thickness, 36 mm width with an EDM side-groove. The effective thickness of CT-3 after the EDM machining was 3 mm, which means that the crack would be assisted from both sides with the 0.5 mm deep cut. The determined results of J-values for this steel yield for the specimen with $B = 4$ mm 275 N/mm, for $B = 25$ mm 140 N/mm, and for B effective = 3 mm with the EDM side-groove 50 N/mm. The specimen having an EDM side-groove obeys the required straight crack profile after the fracture and yield to a valid provisional critical J-value considering the ASTM E 813 paragraphs 9.4.1.5 and 9.4.1.6. However, the size requirement with 4.5 mm ($B > 25 \cdot J_{IC} / \text{yield strength}$) exceeds in a small extent the used specimens thickness, which means that the determined value is at borderline.

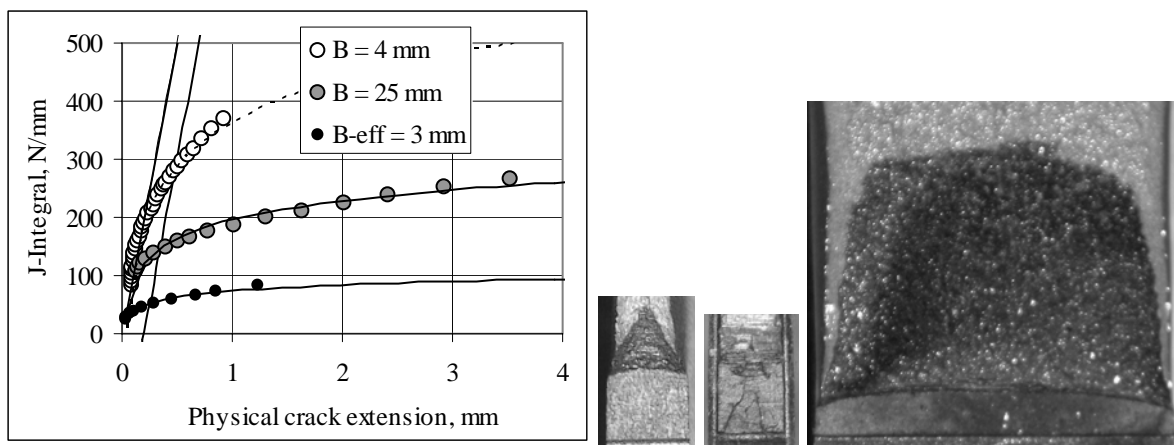


FIGURE 7. Resistance curve of a C-steel material (ST 52, Werkstoff No: 1.0570) measured at 295 K shows the results of the three specimens of different size (diagram at left). The images at right show the fracture appearance of the measured 3 specimens starting from far left with 4 mm thick CT, 4 mm thick (however, with an EDM side-groove with $B = 3$ mm effective thickness) CT, and 25 mm thick CT.

Conclusions

The obtained recent investigation results of high toughness stainless steel materials and aluminum alloys with respect to critical J are scrutinized and the resistance curves of those are analyzed. The main goal of these investigations was to present a reasonable solution to handle the often observed virtual negative crack extensions during the loading of the compact tension specimens. The derived function of the stiffness versus onset of the unloading displacement data, which was obtained by ASTM E 813 standard single specimen compliance technique show in majority of the cases especially for high toughness materials a clear maximum. This maximum has been identified to be the crack initiation position of the material under test. The reason of the parabolic shaped function has been attributed to the two opposing effects. These were; firstly, the start of the crack tip blunting resulting to a stiffness increase because of strain hardening of the plastic zone and secondly, the start of crack initiation, after which the stiffness decreases gradually. Furthermore, measurements confirm that an EDM side-groove technique avoids the crack tunneling and this technique is superior compared to the recommended machine side-grooving. Using a high toughness cryogenic cast stainless steel and a standard carbon steel material it could be shown that an EDM side-groove assists the crack extension procedure in an ideal way to accomplish a straight crack profile, fulfilling the required ASTM standard's criterion.

References

1. ASTM E399-83, Standard Test Method for Plane-Strain Fracture Toughness of Metallic Materials, *Annual book of ASTM Standards*, Vol. 03.01, Philadelphia (1983)
2. ASTM E813-81, Standard Test Method for J_{IC} , a Measure of Fracture Toughness, *Annual book of ASTM Standards*, Vol. 03.01, Philadelphia (1986)
3. ASTM E813-88, Standard Test Method for J_{IC} , a Measure of Fracture Toughness, *Annual book of ASTM Standards*, Vol. 03.01, Philadelphia (1988)
4. Rosenthal Y. A., Tobler R. L., and Purtscher P. T., *JTEVA*, 18 (4), 1990, pp. 301-304
5. Seok C., *International Journal of Fracture*, **102**: 2000, pp. 259-269
6. Nyilas A., Shibata K, Specking W., and Kiesel H., *Advances in Cryogenic Engineering (Materials)* 46A, edited by U. B. Balachandran *et al.*, Plenum Press, New York, 2000, pp. 81-88
7. Nishimura A., Yamamoto J, and Nyilas A., *Advances in Cryogenic Engineering (Materials)* 44A, edited by U. B. Balachandran *et al.*, Plenum Press, New York, 1998, pp. 145-152
8. JIS Z 2284:1998, Method of elastic-plastic fracture toughness J_{IC} testing for metallic materials in liquid helium, *Japanese Standard Association 2000*
9. Nyilas A. Obst B., and Harries D. R., *Advances in Cryogenic Engineering (Materials)* 44A, edited by U. B. Balachandran *et al.*, Plenum Press, New York, 1998, pp. 17-24
10. Nishimura A., Yamamoto J, and Nyilas A., *Advances in Cryogenic Engineering (Materials)* 44A, edited by U. B. Balachandran *et al.*, Plenum Press, New York, 1998, pp. 81-88
11. Sugano M., Osamura. K, and Nyilas A., *Supercond. Sci.Tecnol.* **16** (2003), pp 1064-1070